

Integrated nanotube circuits: Controlled growth and ohmic contacting of single-walled carbon nanotubes

Hyongsok T. Soh and Calvin F. Quate^{a)}

E. L. Ginzton Laboratory, Stanford University, Stanford, California 94305-4085

Alberto F. Morpurgo and Charles M. Marcus^{b)}

Department of Physics, Stanford University, Stanford, California 94305-4060

Jing Kong and Hongjie Dai^{c)}

Department of Chemistry, Stanford University, Stanford, California 94305-5080

(Received 12 February 1999; accepted for publication 4 June 1999)

Single-walled carbon nanotubes are synthesized by chemical vapor deposition of methane at controlled locations on a substrate using patterned catalytic islands. The combined synthesis and microfabrication technique presented here allows a large number of ohmically contacted nanotube devices with controllable length to be placed on a single substrate. Transport studies demonstrate ohmic contacting, giving two-terminal resistances as low as 20 k Ω at low temperatures. © 1999 American Institute of Physics. [S0003-6951(99)01331-5]

A strong interest in the electrical properties of carbon nanotubes derives both from their unique status as an atomically well-defined one-dimensional system, allowing experimental studies of band structure,¹⁻⁷ electron-electron interactions,⁸ electron-lattice coupling^{9,10} and electron localization,^{10,11} as well as from their potential as the basis of nanometer-scale electronic devices. For instance, metallic-semiconducting junctions within single-walled nanotubes (SWNTs) may lead to transistors and Schottky rectifiers within a single molecule.^{12,13}

While there has been considerable progress in understanding the electrical properties of nanotubes, as well as exploring their possible applications,¹⁴⁻¹⁶ what has been lacking is an efficient strategy for integrating nanotubes into electronic structures. In particular, it would be desirable from both a scientific and technological point of view to control not only the diameter and chirality of a SWNT, but also its length, position, and orientation. It is equally desirable to develop a means of making robust, low-resistance electrical contact between nanotubes and metallic electrodes. These goals pose challenges to nanotube synthesis, processing and assembly strategies.

Recently, we developed a chemical vapor deposition (CVD) method to synthesize high quality SWNTs on catalytically patterned surfaces.¹⁷ This technique readily yields large numbers of SWNTs at specified locations, and allows some of the goals described above to be addressed. In this letter, we combine this synthesis method with microfabrication techniques to obtain many nanotube-based electrical circuits on a single substrate with controllable positions and length (ranging from 300 nm to 10 μm), and to connect the tube to macroscopic electrodes. We find that the contacts formed in this way often have very low resistance, of order

of the quantum of resistance (tens of kilohms) even at low temperatures.

The fabrication process involves three steps of electron beam lithography (EBL) using polymethylmethacrylate (PMMA) as the resist. Si wafers with 1 μm thick thermally grown SiO₂ were used as substrates. In the first step, Ti/Au (10 nm/60 nm) alignment marks are patterned by EBL and liftoff [Fig. 1(a)]. In the second step, 12 groups of patterns, each consisting 5 pairs of regularly spaced 5 μm \times 5 μm squares, are defined in PMMA [Fig. 1(b)] by EBL. After development, a few drops of the suspended catalyst material is placed on the surface of the substrate, filling the exposed PMMA "petri-dishes." After the solvent dries, the remaining PMMA is removed, leaving patterned catalyst islands [Fig. 1(c)]. Nanotubes are then synthesized by methane

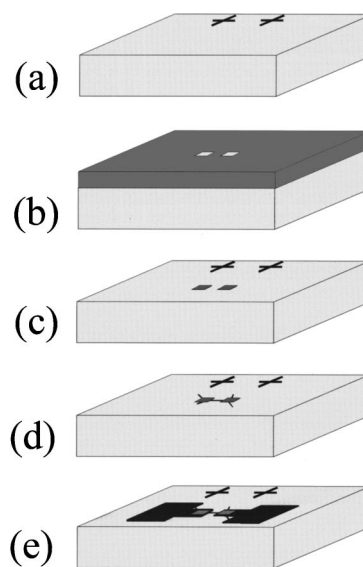


FIG. 1. Schematic of process steps: (a) patterning of Ti/Au alignment-marks on the substrate; (b) patterning of 5 μm \times 5 μm "petri-dishes" in PMMA; (c) catalyst deposition followed by PMMA liftoff in 1,2-dichloroethane; (d) CVD synthesis; and (e) final device with metallic electrodes.

^{a)}Electronic mail: quate@ee.stanford.edu

^{b)}Electronic mail: cmarcus@leland.stanford.edu

^{c)}Electronic mail: hdai@chem.stanford.edu

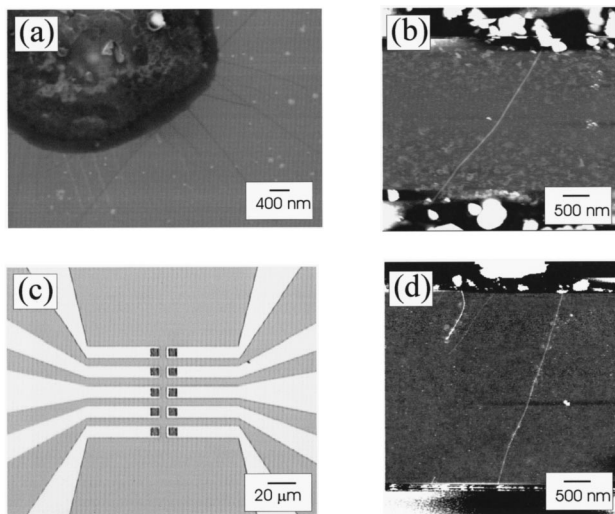


FIG. 2. (a) SEM image showing SWNTs (dark lines) grown off a catalyst islands. (b) AFM image of an individual SWNT bridging two catalyst islands. (c) Optical micrograph of a set of devices containing five pairs of islands (dark squares) with electrodes. (d) AFM image of a SWNT bridging two metal pads in a finished device.

chemical CVD [Fig. 1(d)]. The third EBL step, following CVD synthesis, is to place electrical contact pads (Ti 15 nm/Au 60 nm) over the catalyst islands. The contact pads fully covered the islands and extended over their edges by $\sim 0.5 \mu\text{m}$ [Fig. 1(e)].

The detailed growth procedure is given in Ref. 17. Briefly, the catalyst consists of 15 mg of alumina nanoparticles, 0.05 mmol $\text{Fe}(\text{NO}_3)_3 \cdot 9\text{H}_2\text{O}$ and 0.015 mmol $\text{Mo}_2(\text{acac})_2$ in 15 ml of methanol. The catalyst is stirred for 24 h and sonicated for 1 h before being deposited on the patterned PMMA [Fig. 1(c)]. CVD synthesis is carried out for 10 min at 900°C in a 1 in. diameter tube furnace using a methane flow rate of $5000 \text{ cm}^3/\text{min}$. Under these conditions, nanotubes grown from the catalyst islands are predominantly individual SWNTs with few structural defects;^{17,18} a small quantity of SWNT ropes (diameter $> 5 \text{ nm}$) is also present.

Scanning electron microscope (SEM) and atomic force microscope (AFM) micrographs of SWNTs growing from catalyst islands are shown in Figs. 2(a) and 2(b). SWNT bridging two islands [Figs. 2(b) and 2(d)] are frequently observed.¹⁷ A nanotube bridge forms when a tube growing from one catalyst island falls on and interacts with another island during CVD synthesis.¹⁷ The interaction between tube island and tube substrate is mechanically strong,¹⁷ allowing the nanotube to withstand mechanical forces in subsequent lithographic processing.

By setting the separation between the catalytic islands, we are able to control the length of nanotubes used for transport measurements. The lengths of the individual SWNTs that we have measured were in the range of $0.3\text{--}10 \mu\text{m}$. Figure 2(d) shows a SWNT connecting two metal pads. When the pads are closely spaced ($< 1 \mu\text{m}$), multiple tubes tend to bridge the gap. Using an AFM tip, we are able to cut nanotubes mechanically or electrically until a single tube remained.¹⁹

Circuits formed by nanotube bridges between islands and metal electrodes are first characterized at room temperature by measuring electrical resistance (with a 10 mV voltage

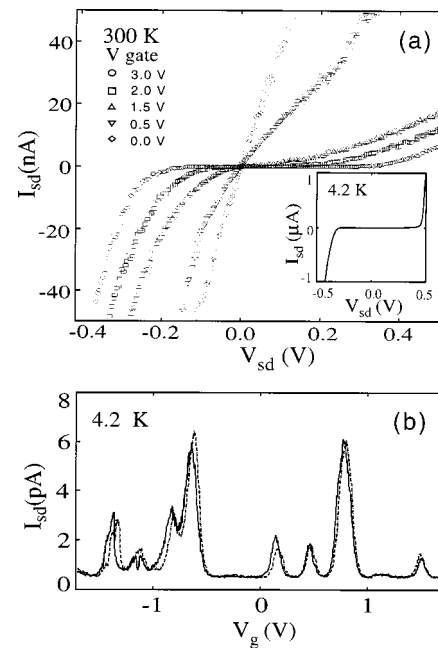


FIG. 3. (a) I - V curves of a semiconducting SWNT for different values of gate voltage (V_g) measured at room temperature. Inset: I - V curve ($V_g = 0$) at 4.2 K. (b) I_{sd} as a function of V_g of a metallic SWNT exhibiting Coulomb oscillations at 4.2 K, measured using a lock-in amplifier with $V_{ac} = 200 \mu\text{V}$ at 17 Hz. The reproducibility of the two traces shows the stability of the sample over small V_g scans.

bias) using a probe station (Signatone, model S-1160). Resistances ranging from $20 \text{ k}\Omega$ to several $\text{M}\Omega$ are normally observed. We find that the lower resistance tubes tend to remain good conductors at low temperatures. After this initial probing, an AFM is used to image the circuits of interest. We have concentrated our transport measurements on individual SWNTs with diameters in the range of $1.0\text{--}1.6 \text{ nm}$ based on AFM data.

Figures 3(a) and 3(b) show transport results for a semiconducting SWNT and a metallic SWNT, both ~ 5 and $3 \mu\text{m}$ long. The I - V curves for the semiconducting SWNT [Fig. 3(a)] were taken at room temperature at various side-gate voltages. The side-gate electrode in this case was one of the metal pads adjacent to the nanotube circuit being measured, about $4 \mu\text{m}$ away. At zero gate voltage ($V_g = 0$), the source-drain current (I_{sd}) of the semiconducting tube depended linearly on the source-drain voltage bias (V_{sd}). However, a strong nonlinearity developed when the gate electrode was biased to a positive voltage with respect to the tube. Increasing V_g resulted in a complete suppression of the linear conductance (5 to 6 order of magnitude suppression at $V_g = +3 \text{ V}$). Negative gate voltages slightly increased the conductance of the semiconducting nanotube, saturating at $V_g \sim -2 \text{ V}$. These results are consistent with field-effect-transistor behavior of semiconducting nanotubes reported by Tans *et al.*¹⁶ and Martel *et al.*²⁰

The low-temperature (4.2 K) I - V curves for the semiconducting tube at $V_g = 0$ [Fig. 3(a), inset] clearly shows the presence of a gap of $\sim 0.8 \text{ eV}$. This indicates that the Fermi level at this temperature is located between the valence and the conduction band, instead of being pinned to the valence band edge as was proposed in Ref. 16. A small asymmetry in the low-temperature I - V curve is presumably due to differ-

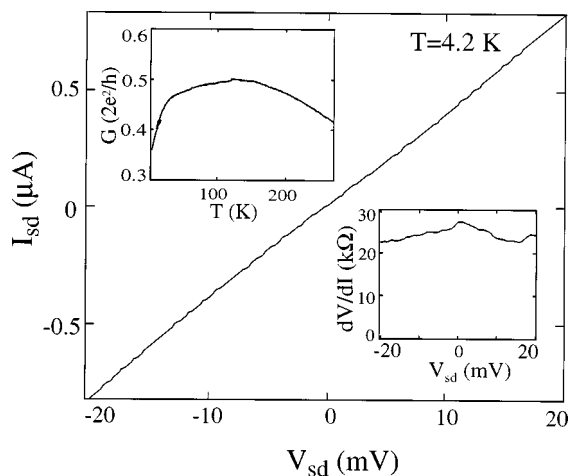


FIG. 4. I - V curve of an individual SWNT exhibiting low two-terminal resistance (~ 20 k Ω) at 4.2 K. Upper inset: Conductance, G , in units of $2e^2/h$, as a function of temperature, T . Lower inset: differential resistance, dV/dI , of the same tube as a function of source-drain voltage V_{sd} .

ences in electrical contact resistance between the SWNT and the two metal electrodes.

Figure 3(b) shows regularly spaced Coulomb blockade oscillations as a function of V_g , observed at 4.2 K in a tube with relatively high resistance, roughly 1 M Ω (as measured at high bias). These data for the high-resistance tubes are similar to what has been seen in previous experiments.^{14,15} These data were obtained using ac voltage bias of 200 μ V and a range of V_g from -1.7 to 1.7 V. Often, however, the two-terminal resistance of the SWNT circuit is much lower, as low as 20 k Ω , and does not show Coulomb blockade oscillations as a function of V_g down to 1.7 K.

The I - V curve of an individual SWNT with low two-terminal resistance at 4.2 K is shown in Fig. 4. This I - V curve is essentially linear with differential resistance showing a very slight increase at zero bias. The upper inset of Fig. 4 shows the temperature dependence of the linear conductance. Conductance depends only weakly on temperature, showing a downward turn $T \sim 50$ K. This weak temperature dependence is generally regarded as the signature of a metallic SWNT.¹⁰ We did not observe Coulomb blockade oscillations with this nanotube at the lowest temperature reached in our experiment (1.7 K). Assuming that transport in the SWNT is ballistic then the measured ~ 20 k Ω two-terminal resistance is due to contact resistances (i.e., ~ 10 k Ω per contact). The fact that this contact resistance is below h/e^2 is consistent with the absence of Coulomb blockade.

The synthesis and fabrication process reported here al-

lows large numbers of integrated nanotube circuits to be built reliably. It also provides contact resistances roughly 100 times lower than can be obtained by placing contacts either on top of or below randomly located tubes, which previously was the state of the art.^{14,15} Important problems that remain to be addressed include understanding the precise nature of the interfaces between nanotube metal or nanotube-catalyst metal and their relations to the low resistance ohmic contact, and a means of controlling the chirality of the nanotube.

This work was supported by DARPA/ETO, National Science Foundation PECASE program (DMR-9629180-1), National Science Foundation Partnership for Nanotechnology program (ECS-9871947), Stanford Center for Materials Research (an NSF-MRSEC), National Nanofabrication Users Network (funded by National Science Foundation ECS-9731294), the Camille Henry-Dreyfus Foundation and American Chemical Society.

- ¹M. S. Dresselhaus, G. Dresselhaus, and P. C. Eklund, *Science of Fullerenes and Carbon Nanotubes* (Academic, San Diego, 1996).
- ²T. W. Ebbesen, *Phys. Today* **49**, 26 (1996).
- ³R. Saito, M. Fujita, G. Dresselhaus, and M. S. Dresselhaus, *Appl. Phys. Lett.* **60**, 2204 (1992).
- ⁴N. Hamada, S. Sawada, and A. Oshiyama, *Phys. Rev. Lett.* **68**, 1579 (1992).
- ⁵J. W. Mintmire, B. I. Dunlap, and C. T. White, *Phys. Rev. Lett.* **68**, 631 (1992).
- ⁶T. Odom, J. Huang, P. Kim, and C. M. Lieber, *Nature (London)* **391**, 62 (1998).
- ⁷J. W. G. Wildoer, L. C. Venema, A. G. Rinzler, R. E. Smalley, and C. Dekker, *Nature (London)* **391**, 59 (1997).
- ⁸C. Kane, L. Balents, and M. P. A. Fisher, *Phys. Rev. Lett.* **79**, 5086 (1997).
- ⁹C. L. Kane and E. J. Mele, *Phys. Rev. Lett.* **78**, 1932 (1997).
- ¹⁰C. L. Kane, E. J. Mele, R. Lee, J. E. Fischer, P. Petit, H. Dai, A. Thess, R. E. Smalley, A. R. M. Verschuereen, S. J. Tans, and C. Dekker, *Europhys. Lett.* **6**, 683 (1998).
- ¹¹C. T. White and T. N. Todorov, *Nature (London)* **393**, 240 (1998).
- ¹²L. Chico, V. H. Crespi, L. X. Benedict, S. G. Louie, and M. L. Cohen, *Phys. Rev. Lett.* **76**, 971 (1996).
- ¹³P. G. Collins, A. Zettl, H. Bando, A. Thess, and R. E. Smalley, *Science* **278**, 100 (1997).
- ¹⁴S. J. Tans, M. H. Devoret, H. Dai, A. Thess, R. E. Smalley, L. J. Geerligs, and C. Dekker, *Nature (London)* **386**, 474 (1997).
- ¹⁵M. Bockrath, D. H. Cobden, P. L. McEuen, N. G. Chopra, A. Zettl, A. Thess, and R. E. Smalley, *Science* **275**, 1922 (1997).
- ¹⁶S. Tans, A. Verschuereen, and C. Dekker, *Nature (London)* **393**, 49 (1998).
- ¹⁷J. Kong, H. Soh, A. Cassell, C. F. Quate, and H. Dai, *Nature (London)* **395**, 878 (1998).
- ¹⁸J. Kong, A. M. Cassell, and H. Dai, *Chem. Phys. Lett.* **292**, 567 (1998).
- ¹⁹J. Kong and H. Dai (unpublished results).
- ²⁰R. Martel, T. Schmidt, H. R. Shea, T. Hertel, and P. Avouris, *Appl. Phys. Lett.* **73**, 2447 (1998).